163–169 (2000).
8. Rando, N. *et al.* S-cam: A spectrophotometer for optical astronomy: Performance and latest results. *Rev. Sci. Instrum.* **71**(12), 4582–4591 (2000).
9. Twerenbold, D. Giaever-type superconducting tunneling junctions as high-resolution X-ray-detectors. *Europhys. Lett.* **1**(5), 209–214 (1986).
10. Kraus, H. *et al.* High-resolution X-ray-detection with superconducting tunnel-junctions. *Europhys. Lett.* **1**(4), 161–166 (1986).
11. Irwin, K., Hilton, G., Wollman, D. & Martinis, J. X-ray detection using a superconducting transition-edge sensor microcalorimeter with electrothermal feedback. *Appl. Phys. Lett.* **69**(13), 1945–1947 (1996).
12. Irwin, K. *et al.* A Mo-Cu superconducting transition-edge microcalorimeter with 4.5 eV energy resolution at 6 keV. *Nucl. Instrum. Meth. A* **444,** 184–187 (2000).
13. Angloher, G. *et al.* Energy resolution of 12 eV at 5.9 keV from Al superconducting tunnel junction detectors. *J. Appl. Phys.* **89,** 1425–1429 (2001).
14. Li, L. *et al.* Improved energy resolution of X-ray single photon imaging spectrometers using superconducting tunnel junctions. *J. Appl. Phys.* **90,** 3645–3647 (2001).
15. Chervenak, J. *et al.* Superconducting multiplexer for arrays of transition edge sensors. *Appl. Phys. Lett.* **74,** 4043–4045 (1999).
16. Yoon, J. *et al.* Single superconducting quantum interference device multiplexer for arrays of low-temperature sensors. *Appl. Phys. Lett.* **78,** 371–373 (2001).
17. Mazin, B. A., Day, P. K., Leduc, H. G., Vayonakis, A. & Zmuidzinas, J. Superconducting kinetic inductance photon detectors. *Proc. SPIE* **4849,** 283–293 (2002).
18. Tinkham, M. *Introduction to Superconductivity*, 2nd edn (McGraw-Hill, New York, 1996).
19. Kozorezov, A. G. *et al.* Quasiparticle-phonon downconversion in nonequilibrium superconductors. *Phys. Rev. B* **61** (May), 11807–11819 (2000).
20. Mattis, D. C. & Bardeen, J. Theory of the anomalous skin effect in normal and superconducting metals. *Phys. Rev.* **111,** 412–417 (1958).
21. Moseley, S., Mather, J. & McCammon, D. Thermal detectors as x-ray spectrometers. *J. Appl. Phys.* **56,** 1257–1262 (1984).
22. Wilson, C., Frunzio, L. & Prober, D. Time-resolved measurements of thermodynamic fluctuations of the particle number in a nondegenerate Fermi gas. *Phys. Rev. Lett.* **87,** 067004 (2001).
23. Sergeev, A., Mitin, V. & Karasik, B. Ultrasensitive hot-electron kinetic-inductance detectors operating well below the superconducting transition. *Appl. Phys. Lett.* **80,** 817–819 (2002).
24. Zmuidzinas, J. & LeDuc, H. G. Quasi-optical slot antenna SIS mixers. *IEEE Trans. Microwave Theory Tech.* **MTT-40,** 1797–1804 (1992).
25. Li, L., Frunzio, L., Wilson, C. & Prober, D. Quasiparticle nonequilibrium dynamics in a superconducting Ta film. *J. Appl. Phys.* **93,** 1137–1141 (2003).
26. Chang, W. Inductance of a superconducting strip transmission-line. *J. Appl. Phys.* **50,** 8129–8134 (1979).
27. McMillan, W. Transition temperature of strong-coupled superconductors. *Phys. Rev.* **167,** 331–334 (1968).
28. Wells, G. L., Jackson, J. E. & Mitchell, E. N. Superconducting tunneling in single-crystal and polycrystal films of aluminum. *Phys. Rev. B* **1,** 3636–3644 (1970).
29. Kaplan, S. *et al.* Quasiparticle and phonon lifetimes in superconductors. *Phys. Rev. B* **14,** 4854–4873 (1976).

Acknowledgements This work has been supported in part by NASA (Aerospace Technology Enterprise), the JPL Director's Research and Development Fund, and the Caltech President's Fund. We are grateful for the support of A. Lidow, Caltech Trustee.

Competing interests statement The authors declare that they have no competing financial interests.

Correspondence and requests for materials should be addressed to P.K.D. (Peter.K.Day@jpl.nasa.gov).

Imaging coexisting fluid domains in biomembrane models coupling curvature and line tension

Tobias Baumgart[1], Samuel T. Hess[2] & Watt W. Webb[1]

[1]*Applied and Engineering Physics, Cornell University, Ithaca, New York 14853, USA*
[2]*Laboratory of Cellular and Molecular Biophysics, National Institute of Child Health and Human Development, National Institutes of Health, Bethesda, Maryland 20892, USA*

Lipid bilayer membranes—ubiquitous in biological systems and closely associated with cell function—exhibit rich shape-transition behaviour, including bud formation[1] and vesicle fission[2]. Membranes formed from multiple lipid components can laterally separate into coexisting liquid phases, or domains, with distinct compositions. This process, which may resemble raft formation in cell membranes, has been directly observed in giant unilamellar vesicles[3,4]. Detailed theoretical frameworks[5–11] link the elasticity of domains and their boundary properties to the shape adopted by membranes and the formation of particular domain patterns, but it has been difficult to experimentally probe and validate these theories. Here we show that high-resolution fluorescence imaging using two dyes preferentially labelling different fluid phases directly provides a correlation between domain composition and local membrane curvature. Using freely suspended membranes of giant unilamellar vesicles, we are able to optically resolve curvature and line tension interactions of circular, stripe and ring domains. We observe long-range domain ordering in the form of locally parallel stripes and hexagonal arrays of circular domains, curvature-dependent domain sorting, and membrane fission into separate vesicles at domain boundaries. By analysing our observations using available membrane theory, we are able to provide experimental estimates of boundary tension between fluid bilayer domains.

We study giant unilamellar vesicles (GUVs) formed from a ternary mixture of the lipids sphingomyelin, dioleoylphosphatidylcholine (DOPC) and cholesterol[3]. Sphingomyelin and cholesterol enrich in a liquid phase with short-range order (L_o), and DOPC prefers a disordered liquid (L_d) phase. The phase diagram of this lipid mixture at physiologically relevant temperatures shows a large binary coexistence region of L_o and L_d domains (A.K. Smith and G.W. Feigenson, personal communication; see also Supplementary Information for further details). Figure 1 presents images of equatorial sections of GUVs (obtained using two-photon microscopy), exhibiting phase coexistence of the L_o (blue) + L_d (red) phases at varying compositions. Figure 1a–d shows shapes with symmetry around an axis in the vertical direction within the image plane.

The geometry of phase-separated vesicles is theoretically obtained by minimizing an energy functional with contributions arising from bending resistance, lateral tensions, line tension and normal pressure difference. The bending energy F_b of an axially symmetric lipid membrane has components arising from mean curvature (first term) and Gauss curvature[12,13] (second term), and is summed over every domain i of the vesicle[8]:

$$F_b^i = \frac{\kappa^i}{2}\int_{A^i}\left(C_m + C_p - C_0\right)^2 dA + \kappa_G^i \int_{A^i} C_m C_p dA \qquad (1)$$

Here κ, κ_G, C_m and C_p are mean and Gauss bending rigidities and principal curvatures along the meridians and parallels, respectively, and the integral is extended over all domain areas i. C_0 is a curvature preference, which is often assumed to be constant within a domain[5,8,11] but can in general vary locally[14]. The bending modulus κ typically has a value of $\sim 10^{-19}$ J (ref. 15). The second term in equation (1) influences the vesicle shape only if κ_G^i values differ between domains i (ref. 8).

Comparison of Fig. 1a and 1b, which show similar shapes even though the domains are reversed, suggests that bending resistance differences (or any curvature preferences) are not dominant in determining global vesicle shapes. In fact, a line tension σ at the boundaries between coexisting fluid membrane domains has been proposed to control membrane deformation, budding and fission[5]. Theoretical estimates of σ are of the order of 10^{-11} N for systems far from[5] critical points of the lipid phase diagram, and σ vanishes at critical points[5,16]. Above a limiting boundary length $S^0 \approx 8\kappa/\sigma \approx 80$ nm, an initially flat domain would transform into a complete spherical bud with vanishing neck radius, provided that sufficient membrane area is available[5]. Accordingly, the domain boundary radii observed in Fig. 1 favour bud formation even for much smaller estimates of σ.

This simplifying theoretical description neglects the constraints on membrane domain areas and surface-to-volume ratio (s/v), which are constant on the timescale of our experiment (up to

© 2003 Nature Publishing Group

1 h), and also neglects the membrane geometry in the neck region of a budded domain. We show (see Supplementary Information) that for liposomes such as shown in Fig. 1, line tension drives vesicles into a shape close to a limit shape characterized by a minimum domain boundary radius R_b. This limit shape consists of truncated spheres, connected at the phase boundary, with areas and volumes of the spherical caps determined by the constrained vesicle volume and domain areas. A further transition into a shape with vanishing neck radius (with vanishing mean curvature and line energy) is suppressed by a lateral membrane domain tension Σ^i. According to Fig. 1a, b and g, the meridional radius of curvature in the neck region is close to the limit of optical resolution. Many of the vesicles we analysed, however, suggest a high, but finite reverse meridional curvature in this region (see, for example, Fig. 1b inset) with a continuous membrane geometry (as opposed to a kink), a reasonable assumption for domain boundaries of finite thickness within fluid membranes. In the neck region, L_d domains bend towards the L_o domains (as shown, for example, in Fig. 1b and g), suggesting smaller bending rigidities κ of L_d compared to L_o phases[15]. The smaller rigidity (or higher flexibility) of L_d phases agrees with our observation that the L_o phase exhibits smaller amplitudes of thermally excited out-of-plane undulations[15,17].

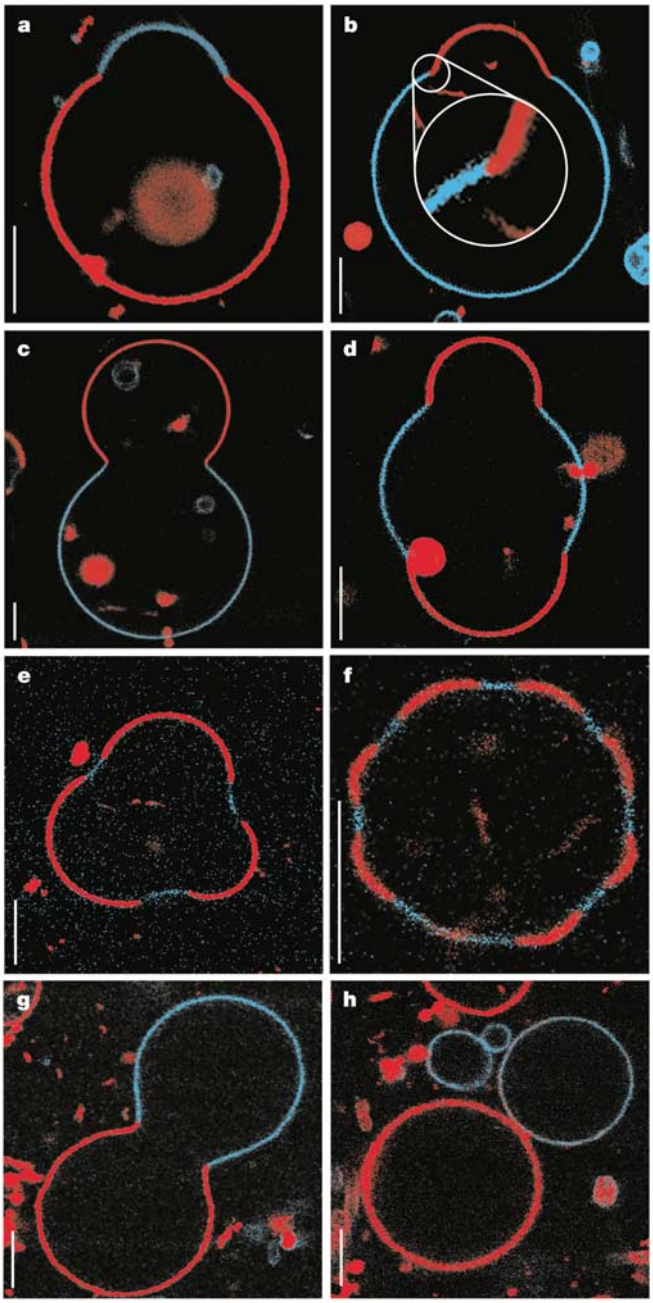

Figure 1 Two-photon microscopy images showing equatorial sections of GUVs with $L_o + L_d$ phase coexistence. GUVs were labelled with perylene (blue) in L_o phases and rho-DPPE (red) in L_d phases. All images superimpose red and blue channels (for separations, see Supplementary Fig. 1′). Some GUVs contain smaller vesicles and lipid fragments. Images obtained at 25 °C, except for **g** (30 °C) and **h** (35 °C). Inset of **b**, enlarged neck region. Scale bars, 5 μm.

A refined shape theory of Jülicher and Lipowsky[8] allowed us to devise a fitting routine using five free parameters, and to determine mechanical vesicle parameters (see Supplementary Information for details). To establish the fundamental relation between domain composition and mechanical properties requires the currently undetermined tie lines of domain coexistence in the ternary phase diagram of our lipid mixtures. We therefore focus, as an example, on the shape of the vesicle shown in Fig. 1c. There we obtain a line tension $\sigma \approx 9 \pm 0.3 \times 10^{-13}$ N, which is an order of magnitude smaller than Lipowsky's above-mentioned rough estimate, which is based on an estimation of the energetic penalty arising from interfacial free energies of a cut across the lipid bilayer at the phase boundary[5]. However, our experimentally obtained value lies in the range of another theoretical estimate (P. Kuzmin, S. Akimov, F. Cohen and J. Zimmerberg, personal communication), which minimizes the sum of energies from elastic compression/stretching and tilt, and hydrophobic height mismatch between the L_o and L_d membrane phases.

Lateral tensions obtained were $\Sigma^{L_d} \approx 8.2 \pm 0.1 \times 10^{-5}\,\mathrm{mN\,m^{-1}}$ and $\Sigma^{L_o} \approx 1.06 \pm 0.01 \times 10^{-4}\,\mathrm{mN\,m^{-1}}$, balanced by a pressure difference (outer minus inner pressure) of $P \approx -1.83 \pm 0.01 \times 10^{-2}\,\mathrm{N\,m^{-2}}$. The lateral tensions significantly suppress microscopically visible thermally excited out-of-plane undulations[18], consistent with our observations. We obtain $\kappa^{L_o}/\kappa^{L_d} \approx 1.25 \pm 0.60$, again suggesting a slightly higher bending rigidity of L_o phases. In contrast to the above-mentioned fitting parameters, the value of $\kappa^{L_o}/\kappa^{L_d}$ is, however, associated with a high uncertainty. Our fit shows a small systematic deviation, particularly in the neck region, which is readily understood by (1) the uncertainty of the experimental determination of the neck geometry, which is close to the optical resolution, and (2) the simplifying assumptions of the theory[8], that is, a constant membrane composition throughout a domain. In the case of the presence of cone-shaped lipids (like cholesterol), steep local curvature gradients can cause lateral and interleaflet lipid redistribution[14,19] and therefore locally modify the mechanical membrane properties.

If the s/v ratio is further increased, either by changing osmotic stress or by a temperature increase, we observe the formation of complete spherical buds, that is, closure of the neck at the domain edge[20], and the fission into separate vesicles (Fig. 1g, h shows a fission sequence). This occasional shape transition occurs abruptly (timescale less than 0.5 s; see Supplementary Movie), indicating an energy barrier[5,8]. In the case of neck radii R_b approaching molecular dimensions, our experimental estimate of σ indicates that the lateral tension $\Sigma = \sigma/R_b$ will rise to values where membranes are expected to rupture[5]. Indeed, we observe fission at the phase boundary, leaving vesicles that differ in their phase state and relative lipid composition (see Fig. 1h and Supplementary Movie).

In addition to phase-separated vesicles with one spheroidal domain, we find vesicles with two, three and multiple caps (Fig. 1d–f), often coexisting within the same sample (vesicles shown in Fig. 1c–f were prepared from a lipid mixture of the same composition). It is possible that those liposomes with multiple caps lacking a curvature preference are not in a state of global energy minimum, as we frequently observe the dynamics of fusion of domains[4,11,21], which reduces total line energy. In vesicles with

© 2003 Nature Publishing Group

budding domains, however, this fusion step seems to be impeded, because domains tend to repel each other upon approach, avoiding high curvature build-up. Indeed, equatorial section images through GUVs with multiple caps (Fig. 1d–f; in these images the L_o phase is continuous and contains separated spheroidal L_d phase caps), as well as stacks of focal plane images of vesicle hemispheres showing domains of similar size (Fig. 2a and b) reveal approximate long-range ordering patterns of cap-shaped domains. Figure 2a and b shows arrangements into both hexagonal and inverted hexagonal patterns, depending on membrane composition. Long-range ordering of fluid membrane domains is clearly matched by a curvature pattern (Figs 1d–f, and 2a and b).

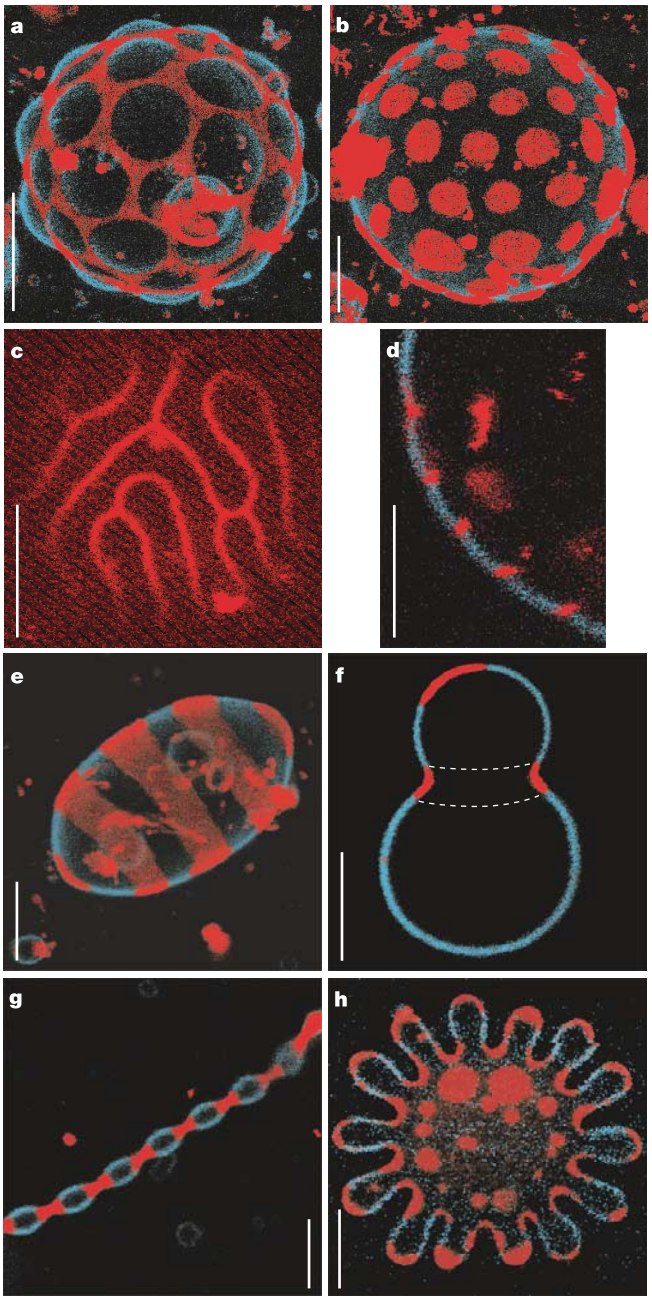

Figure 2 Two-photon microscopy images of GUVs with $L_o + L_d$ phase coexistence. All are superpositions of red and blue channels (for separations see Supplementary Fig. 2′), except **c** (red channel only). **d**, Equatorial section of the same vesicle as in **c**. **a**, **b**, **e**, Hemispherical projections of image stacks taken at 0.5 μm spacing. Image in **c** is focused on vesicle top; **d**, **f**, **g** and **h** show equatorial sections. Dashed lines in **f** indicate an axially symmetric ring domain. Images are obtained at: **a** and **b**, 25 °C; **c** and **d**, 40 °C; **e**, 30 °C; **f**, 25 °C; **g**, 44 °C; **h**, 50 °C. Scale bars, 5 μm.

Domains imaged at room temperature are circular (Fig. 2a and b)[3,4,21]. When temperature was increased to values several degrees below the mixing/demixing transition temperature T_m, in vesicles with and without excess curvature, we observed both L_o phase and L_d phase circular domains to undulate laterally, indicating reduced line tension at higher temperatures. Further temperature increase led to the formation of a homogeneous membrane. Thermally excited lateral domain undulations have normal mean square amplitudes $\langle u_n^2 \rangle = k_B T/(\pi r_o \sigma(n^2 - 1))$, where k_B is Boltzmann's constant, T is temperature, r_0 is the average domain radius and n is the mode number. Accordingly, domains with a radius $r_0 \approx 5\,\mu m$, which visibly undulate with optically resolvable amplitudes, indicate a line tension below $\sigma \approx 10^{-14}$ N (at high temperatures), which is two orders of magnitude smaller than the room-temperature value determined from our shape fitting. In-plane fluctuations of domains at temperatures close to, but below, T_m tend to increase when approaching a composition range (mole fractions of sphingomyelin/DOPC/cholesterol) of 0.63 ± 0.035/0.07 ± 0.035/0.3 ± 0.05. From preliminary data on the temperature dependence of $L_o + L_d$ phase coexistence (see Supplementary Information for further details), we assume this region to be near an upper critical mixing/demixing point, where line tension is expected to decrease as $\sigma \propto (T_c - T)^{\lambda}$ (here T_c is the critical temperature, and the critical exponent $\lambda = 1$; refs 5, 16).

Within this composition range, where L_d phase domains in a continuous L_o matrix are found, at temperatures less than one degree below T_m, in vesicles with excess area (compared to a sphere), the undulating domains tend to assume strongly prolate elliptical shapes; upon further increasing T, a shape instability leads to a stripe-out[7], that is, the formation of numerous thin stripes, with varying (fluctuating) lengths, which rapidly undulate in the plane of the membrane, and can span the whole liposome. We observed multiple stripe domains to arrange into laterally undulating patterns of locally parallel stripes. Close to T_m, scanning microscopy was difficult to apply to image these fluctuating patterns. In favourable cases, however, rapid cooling by several degrees led to a sufficient suppression of stripe pattern undulations (and a slight thickness increase of stripes) that the patterns could be imaged (Fig. 2c). Again, an equatorial section through the same GUV (Fig. 2d) shows a pattern of membrane curvature matching the phase pattern. Two different pattern defects are observed (Fig. 2c), namely the formation of loops and bifurcations with an angle near 120°. The relative thickness of stripes depends on membrane composition and temperature (Fig. 2e).

The stripe-out that we describe here resembles the rippling instability of collapsing bubbles[22], but differs from stripe phase formation in polar lipid monolayers at the air/water interface[23], as the long-range dipolar interaction of zwitterionic lipids is significantly screened in the aqueous environment. Both an increase in total membrane area and the reduced line tension around buds near the main transition temperature will reduce lateral tension within the membrane, and favour the instability described above. Equilibrium stripe phases associated with membrane deformation were also predicted[6,9,10]. Further theoretical study and systematic experiments are clearly required to fully understand the physics of this complex phenomenon. Fusion of the ends of a stripe is frequently observed, which upon cooling (and thereby increasing the line tension) leads to (possibly metastable) liposome-spanning ring domains (Fig. 2e and f), where the line tension dominates the shape of these vesicles.

Homogenous membranes with periodic curvature modulation, such as pearling states in tubular membranes[24] and 'starfish' vesicles[25] at high s/v ratios, have previously been reported. We frequently observed these types of homogeneous membranes at temperatures above T_m. Cooling slightly below T_m leads to the

© 2003 Nature Publishing Group

formation of numerous small domains, which accumulate and fuse into recurrent patterns, suggesting a curvature preference of coexisting domains (Fig. 2g and h). In both cases, the L_d phase is observed to favour saddle shapes, and the high-curvature tip region of the arms of the starfish vesicle (Fig. 2h), which again indicates smaller magnitudes of bending rigidities of L_d phases compared to L_o phase domains, which preferentially segregate into the lower-curvature tubular areas (Fig. 2g and h). Owing to the high temperature and the particular membrane composition, line tension effects are expected to be small in both cases. Note that domains in the essentially flat central body of the starfish vesicle are randomly distributed, as they do not experience a significant curvature gradient.

The experimental approach and observations described here allow us to address two-dimensional critical phenomena, the influence of membrane additives on line tension, and to test and advance theories on membrane shape. Some of our observations may furthermore have analogues in fundamental biological membrane processes[26,27]. □

Methods

Vesicle preparation

GUVs were mostly prepared by the method of electroswelling[28], at a temperature of 60 °C, in a solution of 100 mM sucrose. Using GUVs prepared in 50 mM KCl led to virtually the same phenomena observed at zero ionic strength. Lipid mixtures composed of varying fractions of sphingomyelin (from egg), dioleoylphosphatidylcholine and cholesterol were used. The elevated temperature ensured that GUVs were formed from swollen lipid membranes above the upper critical mixing/demixing temperature of L_o/L_d phase coexistence. The mixing/demixing temperature, T_m, varied with composition (see Supplementary Information for further details). Phase coexistence was observed at temperatures up to 56 ± 0.2 °C.

Fluorescence labelling

GUVs were labelled with two differentially partitioning membrane probes in order to distinguish between L_o and L_d domains. The headgroup labelled lipid probe N-lissamine rhodamine dipalmitoylphosphatidylethanolamine (rho-DPPE) partitioned so effectively into L_d domains that in many cases (depending on the membrane composition) no fluorescence in the coexisting L_o phase domains could be detected. The same behaviour was found for numerous other fluorescence-labelled lipid or fatty acid analogues, including the widely used amphiphilic indocarbocyanine dye DiI. We found that the polycyclic aromatic hydrocarbon dye perylene (among other polycyclic aromatic dyes of similar type) partitions preferentially into the L_o phase. The partitioning is, however, weaker compared to rho-DPPE. Rho-DPPE was added at 1/1,000 (dye/lipid). Perylene was added at 1/500. The only charged component in the lipid mixture used in the present study is the fluorescence probe rho-DPPE. In independent experiments using an uncharged lipid label, we confirmed the occurrence of modulated phases.

Two-photon fluorescence microscopy

Two-photon microscopy was performed as described[29], at $\lambda = 750$ nm, using a 60× water immersion objective. The temperature of GUVs on the microscope stage was controlled by means of a small water bath attached to the objective of an inverted microscope. The microscope objective was additionally kept at constant temperature and thermally isolated from the microscope stage. The temperature variation of our set-up is less than ±100 mK.

Vesicle compositions

Lipid compositions are expressed as mole fractions of sphingomyelin, DOPC and cholesterol, respectively. Vesicles shown in Fig. 1: 1a, 0.25/0.5/0.25; 1b, 0.585/0.1/0.315; 1c–f, 0.45/0.45/0.1; 1g and h, 0.615/0.135/0.25. Vesicles shown in Fig. 2: 2a, 0.56/0.24/0.2; 2b, 0.615/0.135/0.25; 2c and d, 0.675/0.075/0.25; 2e, 0.638/0.112/0.25; 2f, 0.675/0.075/0.25; 2g, 0.63/0.07/0.3; 2h, 0.585/0.102/0.313.

Received 25 March; accepted 19 August 2003; doi:10.1038/nature02013.

1. Käs, J. & Sackmann, E. Shape transitions and shape stability of giant phospholipid vesicles in pure water induced by area-to-volume changes. *Biophys. J.* **60,** 825–844 (1991).
2. Döbereiner, H. G., Käs, J., Noppl, D., Sprenger, I. & Sackmann, E. Budding and fission of vesicles. *Biophys. J.* **65,** 1396–1403 (1993).
3. Dietrich, C. *et al.* Lipid rafts reconstituted in model membranes. *Biophys. J.* **80,** 1417–1428 (2001).
4. Veatch, S. L. & Keller, S. L. Organization in lipid membranes containing cholesterol. *Phys. Rev. Lett.* **89,** 268101 (2002).
5. Lipowsky, R. Budding of membranes induced by intramembrane domains. *J. Phys. II France* **2,** 1825–1840 (1992).
6. Leibler, S. & Andelman, D. Ordered and curved meso-structures in membranes and amphiphilic films. *J. Phys.* **48,** 2013–2018 (1987).
7. Seul, M. & Andelman, D. Domain shapes and patterns: The phenomenology of modulated phases. *Science* **267,** 476–483 (1995).
8. Jülicher, F. & Lipowsky, R. Shape transformations of vesicles with intramembrane domains. *Phys. Rev. E* **53,** 2670–2683 (1996).
9. Andelman, D., Kawakatsu, T. & Kawasaki, K. Equilibrium shape of two-component unilamellar membranes and vesicles. *Europhys. Lett.* **19,** 57–62 (1992).
10. Jiang, Y., Lookman, T. & Saxena, A. Phase separation and shape deformation of two-phase membranes. *Phys. Rev. E* **61,** R57–R60 (2000).
11. Kumar, P. B. S., Gompper, G. & Lipowsky, R. Budding dynamics of multicomponent membranes. *Phys. Rev. Lett.* **86,** 3911–3914 (2001).
12. Helfrich, W. Elastic properties of lipid bilayers: Theory and possible experiments. *Z. Naturforsch.* **28c,** 693–703 (1973).
13. Jenkins, J. T. Static equilibrium configurations of a model red blood cell. *J. Math. Biol.* **4,** 149–169 (1976).
14. Seifert, U. Curvature-induced lateral phase separation in two-component vesicles. *Phys. Rev. Lett.* **70,** 1335–1338 (1993).
15. Duwe, H. P. & Sackmann, E. Bending elasticity and thermal excitations of lipid bilayer vesicles: Modulation by solutes. *Physica A* **163,** 410–428 (1990).
16. Benvegnu, D. J. & McConnell, H. M. Line tension between liquid domains in lipid monolayers. *J. Phys. Chem.* **96,** 6820–6824 (1992).
17. Schneider, M. B., Jenkins, J. T. & Webb, W. W. Thermal fluctuations of large quasi-spherical bimolecular phospholipid vesicles. *J. Phys.* **45,** 1457–1472 (1984).
18. Helfrich, W. & Servuss, R. M. Undulations, steric interactions and cohesion of fluid membranes. *Nuovo Cimento D* **3,** 137–151 (1984).
19. Chen, C.-M., Higgs, P. G. & MacKintosh, F. C. Theory of fission for two-component lipid vesicles. *Phys. Rev. Lett.* **79,** 1579–1582 (1997).
20. Lipowsky, R. & Dimova, R. Domains in membranes and vesicles. *J. Phys. Condens. Matter* **15,** S31–S45 (2003).
21. Samsonov, A. V., Mihalyov, I. & Cohen, F. S. Characterization of cholesterol-sphingomyelin domains and their dynamics in bilayer membranes. *Biophys. J.* **81,** 1486–1500 (2001).
22. Debregeas, G., de Gennes, P.-G. & Brochard-Wyart, F. The life and death of "bare" viscous bubbles. *Science* **279,** 1704–1707 (1998).
23. Andelman, D., Brochard, F. & Joanny, J. F. Phase transitions in Langmuir monolayers of polar molecules. *J. Chem. Phys.* **86,** 3673–3681 (1987).
24. Bar-Ziv, R. & Moses, E. Instability and "pearling" states produced in tubular membranes by competition of curvature and tension. *Phys. Rev. Lett.* **73,** 1392–1395 (1994).
25. Wintz, W., Döbereiner, H. G. & Seifert, U. Starfish vesicles. *Europhys. Lett.* **33,** 403–408 (1996).
26. Mukherjee, S. & Maxfield, F. R. Role of membrane organization and membrane domains in endocytic lipid trafficking. *Traffic* **1,** 203–211 (2000).
27. Huttner, W. B. & Zimmerberg, J. Implications of lipid microdomains for membrane curvature, budding and fission. *Curr. Opin. Cell Biol.* **13,** 478–484 (2001).
28. Mathivet, L., Cribier, S. & Devaux, P. F. Shape change and physical properties of giant phospholipid vesicles prepared in the presence of an AC electric field. *Biophys. J.* **70,** 1112–1121 (1996).
29. Denk, W., Strickler, J. H. & Webb, W. W. Two-photon laser scanning fluorescence microscopy. *Science* **248,** 73–76 (1990).

Supplementary Information accompanies the paper on **www.nature.com/nature**.

Acknowledgements We thank G. W. Feigenson, J. T. Jenkins, G. Gompper, J. Zimmerberg, A. K. Smith and A. T. Hammond for discussions. This work was supported in part by a CMBSTD grant of the W.M. Keck Foundation and an NIBIB-NIH grant to the Developmental Resource for Biophysical Imaging Opto-Electronics.

Competing interests statement The authors declare that they have no competing financial interests.

Correspondence and requests for materials should be addressed to W.W.W. (www2@cornell.edu).

Cool Indonesian throughflow as a consequence of restricted surface layer flow

Arnold L. Gordon, R. Dwi Susanto & Kevin Vranes

Lamont-Doherty Earth Observatory, Columbia University, Palisades, New York 10964, USA

Approximately 10 million $m^3 s^{-1}$ of water flow from the Pacific Ocean into the Indian Ocean through the Indonesian seas[1]. Within the Makassar Strait, the primary pathway of the flow[2], the Indonesian throughflow is far cooler than estimated earlier, as pointed out recently on the basis of ocean current and temperature measurements[3,4]. Here we analyse ocean current and stratification data along with satellite-derived wind measurements, and find that during the boreal winter monsoon, the wind

 © 2003 Nature Publishing Group